

Tunneling Escape Rate of Electrons From Quantum Well in Double-Barrier Heterostructures

M. Tsuchiya, T. Matsusue, and H. Sakaki

Institute of Industrial Science, University of Tokyo, Minato-ku, Tokyo 106, Japan

(Received 30 June 1987)

A tunneling escape rate $1/\tau_T$ of electrons from a single quantum well through thin barriers was successfully determined by measurement and analysis of the lifetime τ_e of electrons generated in 6.2-nm GaAs single quantum wells by a picosecond laser pulse. The measured τ_e was found to decrease systematically as the AlAs barrier thickness L_B was reduced. The τ_e for $L_B < 4$ nm was found to agree very well with the lifetime τ_T predicted from the energy width of the resonance transmission. Irrelevance of coherence versus incoherence in the tunneling escape process is also pointed out.

PACS numbers: 73.40.Gk, 72.20.Jv, 72.80.Ey, 73.40.Lq

Tunneling is one of the basic quantum-mechanical phenomena in ultrathin semiconductor heterostructures. Tunneling through double-barrier (DB) structures with a quantum well (QW) in between¹ has received special attention because of its importance both for practical applications and for the clarification of basic concepts of resonant tunneling. As a result of past investigations, the static features of electron tunneling through DB structure are well clarified.²

In contrast to the static characteristics, the dynamical aspect of DB tunneling is not well explored. Among the most important points to be investigated are the buildup process of electrons inside of QW resonators and the subsequent escape process of electrons, since they are the key processes that govern the ultimate speed of resonant tunneling. Up to now, however, no direct experiment seems to have been done. In this Letter, we report our attempt to determine the tunneling escape rate from QW's in AlAs-GaAs-AlAs DB structures by studying the time-resolved photoluminescence (PL) with a picosecond laser. Note that the tunneling escape is a basic process that takes place in both coherent tunneling and incoherent tunneling.^{3,4}

DB structures studied here are schematically shown in Fig. 1; they were grown on (100) surfaces of semi-insulating GaAs substrate at 600°C by molecular-beam epitaxy. First, we grew a superlattice buffer layer (5 periods of 50-nm GaAs/5-nm Al_{0.3}Ga_{0.7}As) and then a 0.7- μ m-thick GaAs layer to reduce nonradiative recombination centers in the upper epilayers. Subsequently, an AlAs-GaAs-AlAs DB was grown, which was then covered by a GaAs cap layer of 30 nm. The thicknesses L_B of the AlAs barriers in five samples range from 2.8 (10 atomic monolayers) to 6.2 nm (22 atomic monolayers), while the width L_W of the GaAs QW was kept at 6.2 nm. The layer thicknesses were strictly controlled by monitoring of the intensity oscillation of reflection high-energy electron diffraction. To get smooth heterointerfaces, molecular-beam epitaxial growth was interrupted at each interface for 1 min. All epilayers are undoped with an estimated residual acceptor (carbon) concentra-

tion of 10^{14} – 10^{15} /cm³. To investigate the case where the tunneling escape is negligible, we prepared under the identical growth conditions a multiple quantum well (MQW) structure which consists of five 6.2-nm-thick GaAs QW's separated by four 5.1-nm-thick AlAs barriers and sandwiched by two 10-nm-thick AlAs barriers on both ends.

Picosecond dye-laser pulses ($\lambda \approx 750$ nm) were used to generate electron-heavy-hole pairs selectively in the ground subband of QW's by tuning of the energy of excitations, and the subsequent QW emission was monitored. Although excess carriers generated in two GaAs regions outside of AlAs barriers also emit photons, their contribution was rejected by a monochromator. Electrons and heavy holes created in QW's are expected to fall to quasithermal equilibrium states in a very fast (subpicosecond) process of parallel momentum relaxation. Since some of the QW interfaces have monolayer steps which cause the well-width fluctuation, some of these carriers may well migrate along the interface from the higher-quantum-energy region to the adjacent lower-energy region, giving rise to some Stokes shift between the absorption and PL spectra, as will be discussed later. Although these intrasubband energy relaxation processes

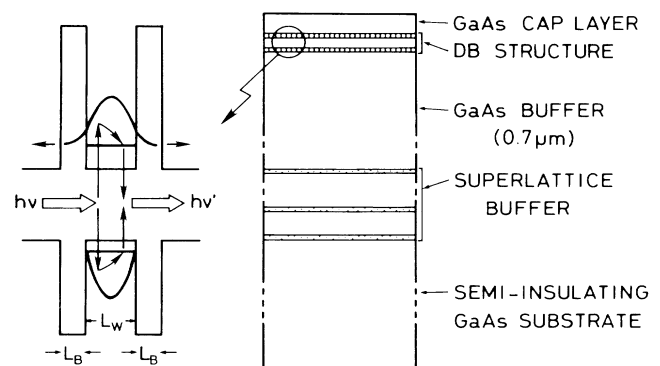


FIG. 1. Schematic structure of AlAs-GaAs-AlAs double-barrier samples used for the present study.

affect the energy distributions, they do not affect the carrier concentration. The only possible mechanisms by which QW carriers are lost are the following three processes: (a) radiative recombination process with nanosecond or subnanosecond time constant, (b) nonradiative recombination process through crystal defects, whose time constant is a nanosecond or longer in higher quality QW's, and (c) tunneling escape process from the GaAs QW to outside through barriers.⁵ Since the effective mass of electrons is much lighter than that of heavy holes, the rate of tunneling escape is calculated to be higher for electrons than for heavy holes by more than 1 order of magnitude. Therefore, the heavy-hole contribution can be neglected in the initial phase of tunneling. We discuss below the PL decay process within QW's right after the excitation laser pulse is turned off.

In case nonradiative recombination processes are negligible, the radiative recombination and the tunneling escape of electrons dominate the decay process of the electron concentration n in QW's; it can be written as

$$dn/dt = -n/\tau_e = -n/\tau_R - n/\tau_T, \quad (1)$$

where $1/\tau_e$, $1/\tau_R$, and $1/\tau_T$ are the total electron-loss rate, the radiative-recombination rate (determined either by excitonic process or bimolecular process, depending on conditions), and the tunneling escape rate. The expected time response of the PL intensity is proportional

to n which is the impulse response of this equation. Since the use of thin and/or low barriers enhances $1/\tau_T$ but does not influence $1/\tau_R$, τ_e will be dominated by the tunneling escape process for thin barriers.

Before investigating τ_e , we have first studied PL spectra and excitation (PLE) spectra at 20 K. Results are shown in Fig. 2. Optical excitation was done by picosecond pulses from the mode-locked dye laser (pulse width ≈ 20 ps, repetition ≈ 41 MHz) pumped by a frequency-doubled Nd-doped yttrium aluminum garnet laser. In PLE spectra, all samples show the well-resolved electron-heavy-hole exciton peak ($e1-hh1$) and the electron-light-hole exciton peak ($e1-lh1$), even when L_B is as thin as 2.8 nm. These well-resolved peaks indicate the stability of excitons as well as high quality of our QW's. Some of these PLE peaks are found to split into two or three subpeaks or exhibit shoulder structures. This reflects the presence of monolayer interface steps with lateral dimension much greater than exciton diameters. These steps were formed during the interruption period of molecular-beam epitaxial growth.⁶ These interface steps also give rise to an appreciable Stokes shift in some QW's, as seen in Fig. 2. Although these well-width fluctuations complicate the assignment of spectral peaks, measured peaks are in good agreement with the Kronig-Penny calculation, in which we find that λ_{e1-hh1} is 765 nm for the exciton binding energy of 10 MeV and that λ_{e1-lh1} is 17 nm shorter than λ_{e1-hh1} .

For the time-resolved PL measurement, the photon energy of the excitation laser was set higher than the $e1-hh1$ transition and lower than the $e1-lh1$ transition as indicated by the arrows in Fig. 2. This prevents any ambiguities in the hole relaxation process from light-hole band to heavy-hole band.

The temporal decay of PL intensity around the main emission peak ($\lambda = \lambda_{\text{peak}} \pm 5$ nm) was measured by a

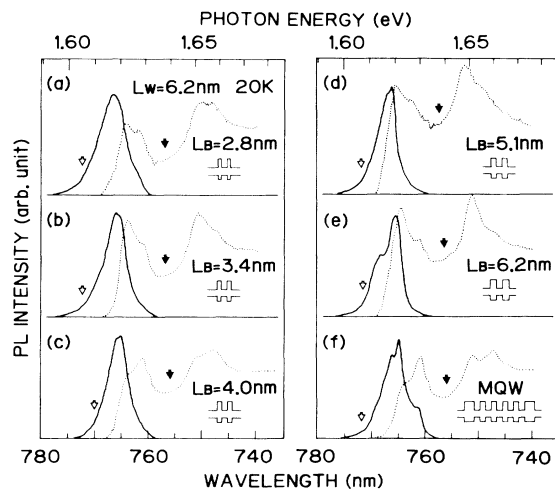


FIG. 2. PL spectra (solid lines) and PLE spectra (dotted lines) of five different DB structures and one MQW sample at 20 K. All the DB samples have the same well width, $L_W = 6.2$ nm, whereas the widths L_B of the AlAs barriers are (a) 2.8, (b) 3.4, (c) 4.0, (d) 5.1, and (e) 6.2 nm, respectively. (f) MQW sample has five periods of 6.2-nm GaAs well separated by 5.1-nm AlAs barrier and is sandwiched by 10-nm-thick AlAs barriers. A filled arrow in each figure shows the wavelength of excitation laser pulse used for the measurement of PL spectra and PL decay rates, whereas an open arrow indicates the detection wavelength for PLE spectra.

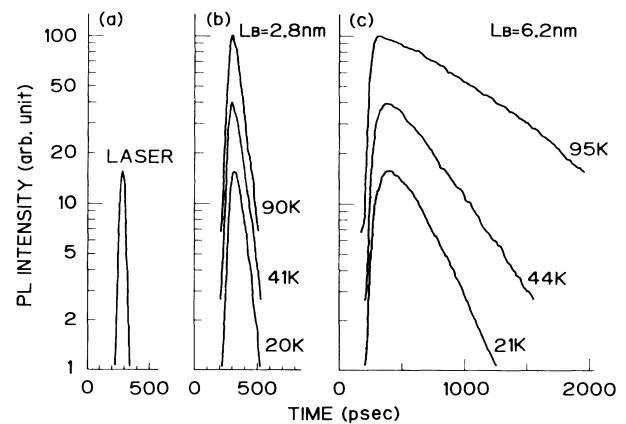


FIG. 3. (a) Temporal evolution of mode-locked dye-laser pulse ($\lambda = 755$ nm), and PL decay of DB samples with (b) $L_B = 2.8$ and (c) 6.2 nm measured at different temperatures by streak camera.

streak camera system (Hamamatsu Photonics) after dispersion of the spectra by a 25-cm grating monochromator; this eliminates any PL components from the GaAs outside of AlAs barriers. The overall time resolution of this system is influenced by such factors as the finite pulse width of optical excitation, the difference of optical lengths in the grating monochromator, and the jitter of the trigger in the streak camera. By our assuming that the impulse response of this extra temporal dispersion is of the Gaussian shape, $\exp(-t^2/T_0^2)$, its net effect can be determined experimentally since it is nearly equal to the observed shape of laser pulses detected by the streak camera through the monochromator. This gives the lower limit to the measurable lifetime ($T_0 \approx 24$ ps).

Figure 3 shows semilogarithmic plots of the measured time evolutions of (a) the excitation dye-laser pulse, (b) the PL from a DB sample with $L_B = 2.8$ nm, and (c) that for $L_B = 6.2$ nm. Figure 3(c) clearly shows that the decay time of PL from a DB with thick barriers increases as temperature θ increases. Although the origin of this θ dependence is not clear at present, it is most likely due to the radiative recombination process, since radiative recombination processes with k -selection rules are generally slowed down at high temperatures.⁷ In contrast, Fig. 3(b) shows that the decay time of PL for $L_B = 2.8$ nm is very short and is nearly independent of θ , indicating that the electron tunneling dominates the decay process. In Fig. 4, the time constants of PL decay are plotted for six samples as functions of θ . Note that the θ dependence weakens as L_B decreases, and nearly disappears at $L_B = 2.8$ nm. Note also that as L_B increases, PL decay times approach asymptotically that of MQW where the tunneling escape process is negligible.

To clarify the dependence of τ_e on L_B , these data are

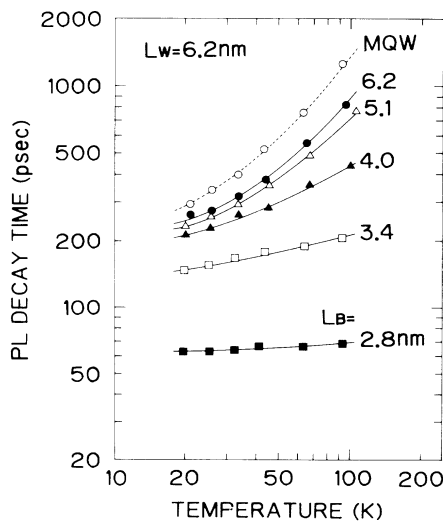


FIG. 4. The temperature dependence of PL decay time with barrier thickness as a parameter.

replotted in Fig. 5 as functions of L_B . Note that the PL decay time, i.e., τ_e , appears to be dominated by at least two different processes, one being nearly independent of L_B and the other strongly dependent on L_B . Since the measured τ_e for $L_B < 4$ nm is exponentially dependent on L_B and independent of θ , the lifetime τ_e in this region is most likely to be dominated by the tunneling escape process and should be nearly equal to the tunneling escape time τ_T . To interpret our result theoretically, we examine the data first within the framework of coherent resonant tunneling, in which both the carrier buildup process and the tunneling escape process are assumed to proceed in a coherent manner. The time delay for each of these processes should be equal to the tunneling time constant τ_T , which can be calculated from the energy width ΔE_{FWHM} of the resonance transmission peak.^{1,5} By assuming a Lorentzian shape of the resonance transmission peak and the Γ -valley barrier height ΔE_C (1.36 eV for the Dingle rule and 0.96 eV for the Miller rule),^{2,5} we have estimated τ_T from $\hbar/(\Delta E_{FWHM}/2)$.¹ The calculated results are shown by the broken line and dot-dashed line in Fig. 5 for two cases and agree very well with the experimental values. Essentially the same conclusion can be reached by our calculating τ_T more simply from the fact that $1/\tau_T$ is given by the product νT of the frequency ν of electron collision with barriers and the tunneling probability T through a single barrier. Since this type of formulation does not assume the coherence of electron waves, τ_T calculated this way should be valid in our case, where $\tau_T (= \tau_e) = 60\text{--}200$ ps)

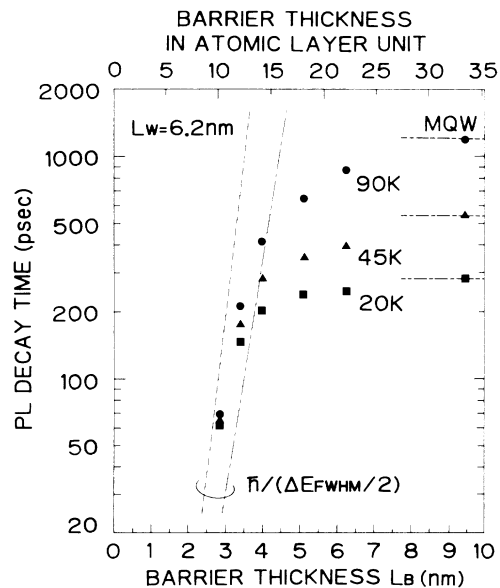


FIG. 5. PL decay times plotted as functions of barrier thickness L_B . When $L_B < 4$ nm, the tunneling escape process is dominant. Broken line and dot-dashed line are theoretical lifetimes calculated by $\hbar/(\Delta E_{FWHM}/2)$, with the assumption that the barrier heights are 1.36 and 0.96 eV, respectively.

is much longer than the mean interval of electron scattering (≤ 1 ps). Hence, we can conclude that the tunneling escape rate is the same for both coherent and incoherent tunneling.⁴

In conclusion, the tunneling escape rate of electrons from QW's has been determined and is shown in excellent agreement with theoretical prediction. Although the full understanding of dynamical aspects of DB tunneling can be completed only when the buildup process of electrons is clarified, the tunneling escape time determined here corresponds to the half of the switching delay in idealized DB resonant tunneling diodes, since the buildup time and the tunneling escape time are roughly the same when devices operate within the complete coherence of electron waves.

The authors wish to express their sincere gratitude to Professor J. Hamasaki, Professor T. Ishihara, Professor T. Sekiguchi, and Professor T. Sugano for their encouragement and to Dr. T. Hiruma and Dr. Y. Tsuchiya of Hamamatsu Photonics for access to the streak camera. This work was supported by a Grant-in-Aid from

the Ministry of Education, Science and Culture, Japan.

¹R. Tsu and L. Esaki, *Appl. Phys. Lett.* **22**, 562 (1973); L. L. Chang, L. Esaki, and R. Tsu, *Appl. Phys. Lett.* **24**, 593 (1974); T. C. L. G. Sollner, W. D. Goodhue, P. E. Tanenwald, C. D. Parker, and D. D. Peck, *Appl. Phys. Lett.* **43**, 588 (1983); E. E. Mendez, W. I. Wang, B. Ricco, and L. Esaki, *Appl. Phys. Lett.* **47**, 415 (1986).

²M. Tsuchiya and H. Sakaki, *Jpn. J. Appl. Phys. Pt. 2* **25**, L185 (1986), and *Appl. Phys. Lett.* **49**, 88 (1986), and **50**, 1503 (1987); E. E. Mendez, E. Calleja, and W. I. Wang, *Phys. Rev. B* **32**, 6026 (1986).

³S. Luryi, *Appl. Phys. Lett.* **47**, 490 (1985).

⁴T. Weil and B. Vinter, *Appl. Phys. Lett.* **50**, 1281 (1987); M. Jonson and A. Gvinchwajg, private communication; M. Buttiker, private communication.

⁵P. J. Price, *Superlattices Microstruct.* **2**, 593 (1986); N. Harada and S. Kuroda, *Jpn. J. Appl. Phys. Pt. 1* **25**, 871 (1986).

⁶M. Tanaka, H. Sakaki, and J. Yoshino, *Jpn. J. Appl. Phys. Pt. 1* **25**, 155 (1986), and *J. Cryst. Growth* **81**, 153 (1987).

⁷T. Matsusue and H. Sakaki, *Appl. Phys. Lett.* **50**, 1429 (1987).